Studies on Chemical and Physical Properties of LiFeMPO$_4$ (M=Cu, La) by Polyol Route

Rasu Muruganantham[1], Marimuthu Sivakumar[2, *], Renganpillai Subadevi[2], Wei-Ren Liu[1]

[1]Energy and Opto-Electronic Materials Lab, Department of Chemical Engineering, Chung Yuan Christian University, Taoyuan City, Taiwan. ROC

[2]Energy Materials Lab, School of Physics, Science Block, Alagappa University, Karaikudi, Tamil Nadu, India

Email address:
murugaphd@yahoo.com (R. Muruganantham), susiva73@yahoo.co.in (M. Sivakumar)
[*]Corresponding author

Abstract: Bare Lithium Iron Phosphate (LiFePO$_4$), Cu, La doped and Cu with La co-doped LiFePO$_4$ composite materials have been prepared via polyol technique without further post heat treatment. The prepared bare and composite materials' crystalline structure has been indexed an orthorhombic phase olivine structure with space group of Pnma. The functional group vibrations and surface morphology of the prepared materials has been observed using Fourier transfer infrared spectroscopy (FT-IR) and scanning electron microscopy (SEM) with EDX analyses. Magnetization measurements revealed that saturation magnetizations (Ms) of the metal doped samples are gradually increased than that of the pure LiFePO$_4$. All the samples exhibit the spin-glass behaviour of magnetic materials.

Keywords: LiFePO$_4$, Cathode Materials, Polyol Process, Magnetic Measurements

1. Introduction

Nowadays, Nanostructure and Nanocrystalline materials have been widely used for different applications such as Energy storage device, Memory device, Bio-medical applications and so on [1, 2]. Lithium-ion batteries are one of the great solutions of energy storage sectors. In this regard, eco-friendly LiFePO$_4$ materials is an attractive cathode material for lithium-ion batteries due to retained the full charge-discharge capacity of the materials and non-toxicity [3]. The LiFePO$_4$ materials has been prepared by several methods via solid state reaction [4], sol-gel [5], carbothermal reduction [6], hydrothermal [7], co-precipitation [8], polyol process [9, 10], solvothermal method [11] etc. Among that, the polyol process is versatile method to produce the economic-energy efficient method compare to other methods. Polyol solvents act as a reducing agent as well as stabilized the prepared materials [9].

Magnetic analysis can be absolute to study magnetic structure and electronic properties of materials used in lithium power sources, i.e., lithium intercalation compounds (Li-ICs). Because, Li ions are nonmagnetic (diamagnetic) and they indirectly affect magnetic properties through manipulate on the cation valence of the 3d iron-transition element. In this context, magnetic properties are of fastidious interest because they are found to be a powerful tool to characterize materials. In particularly, the impurities of nanoparticles cannot be detected by classical analysis like X-ray diffraction (XRD), Fourier transform infrared (FT-IR) spectroscopy, etc. Magnetism is therefore indirectly important to the electrochemical properties of materials [12].

These days, most of the magnetic properties are studied by various techniques such as neutron diffractometry, magnetometry, Nuclear magnetic resonance (NMR), and electron spin resonance (ESR). The microscopic magnetic structure of materials is most often studied by using neutron scattering techniques. More recently, synchrotron sources have been used to study the magnetic scattering. Neutron scattering techniques are currently measured as the most

powerful probe of magnetic materials. The use of superconducting quantum interference devices (SQUID) in ultrasensitive magnetic measurement systems may widely used as a standard technique [12]. Among that the Vibrating Sample Magnetometer (VSM) is one of the appropriate simple techniques to analyze the magnetic properties. Lithium and delithiated lithium iron phosphates are systems where the triphylite LiFe^{2+}PO$_4$ and heterosite Fe^{3+}PO$_4$ phases coexist together with different valence states for the iron ions. In these materials, the structures of two phases are identical and therefore, any differences in the physical or magnetic properties between these two would be related to the lithium percentage [13]. In the mixed-oxide nanoparticles, the magnetization may additionally be affected through the influence of the small sized nanoparticles. The adaptation of the small size nanoparticles led to large surface-to-volume ratio. Santoro and Newman have also reported the magnetic structure of LiFePO$_4$ [14].

Few reports are available for the preparation and characterization of electrochemical performance of Cu-doped LiFePO$_4$ composite [15, 16]. Cho et al [17] reported that the physical and electrochemical properties of La-doped LiFePO$_4$ cathode materials synthesized via a high temperature solid-state method. However, there are no reports available on structural and magnetic properties of single and double metals doped LFP via polyol process.

In this investigation, the first attempt to prepare the Cu, La and co-doped of Cu with La on LiFePO$_4$ via polyol process. The bare and doped LFP composite materials were characterized by structural, morphology, chemical and magnetic properties using X-ray diffraction (XRD), FT-IR, scanning electron microscopy (SEM) with Energy dispersive X-ray spectra (EDX) and vibrating-sample magnetometer (VSM).

2. Experimental Methods

2.1. Synthesis of LiFePO$_4$ and Their Composite Materials Via Polyol Process

Bare and doped-LiFePO$_4$ materials were synthesized by polyol process. The starting precursors of Iron sulphate (FeSO$_4$.7H$_2$O), Lithium hydroxide (LiOH.H$_2$O) and Ammonium dihydrogen phosphate (NH$_4$H$_2$PO$_4$) were taken in stoichiometric amount (1:1:1), which were dissolved in tetra ethylene glycol (TTEG) as a polyol solvent. The dissolved solution was heated to near the boiling point of the polyol solvent (TTEG-315°C) for 12 hours using reflux condenser with round bottom flask. After the reaction, to remove the TTEG and partial organic compounds, the resulting solution was washed several times with acetone. The resulting particles were separated and dried in a vacuum oven at 150°C for 24 h and finally the LiFePO$_4$ particles were obtained. Similarly, 1M of Cu-sulphate and Lanthanum

chloride has been used for single element doped LFP materials. The double elements doped LFP has been maintained 0.5M of Cu and La precursor used to investigate the double doped LFP preparation.

2.2. Characterizations

The Powder X-ray diffraction (PXRD) patterns of LiFePO$_4$ samples were obtained using a PANalytical X'-pert diffractometer (Netherlands) with a Cu K$_\alpha$ radiation operated at 40 kV and 30 mA. The radiation of λ =1.54060 Å in the range of 10-80° was used to determine the crystal structure of the prepared material. The functional group vibration was analyzed using thermo Nicolet 380 FT-IR spectrophotometer by preparing pellets using KBr. The surface morphology of the samples was observed on a scanning electron microscope (SEM) coupled with Energy dispersive X-ray spectra (EDX). The room-temperature magnetic properties of the prepared materials were measured with a vibrating-sample magnetometer (VSM) (Lake Shore 7300 VSM).

3. Results and Discussion

3.1. XRD

Figure 1 shows the XRD pattern of bare and doped LiFePO$_4$ composite materials prepared by polyol process without further heat treatment and special environment. All the diffraction peaks may be indexed to an orthorhombic olivine structure of LiFePO$_4$ with Pnma space group (JCPDS No. 83-2092) without any observable impurity phase. Eventhough, the XRD patterns of all samples are almost same as that of the undoped one and does not affect the phase structure of LFP, which may indicates that the doping concentration is low [19, 20]. The lattice parameter values are calculated and presented in Tab.1. The mean crystallite size has been calculated by Scherrer formula. The crystallite size has been varied with different metal doped on LFP materials.
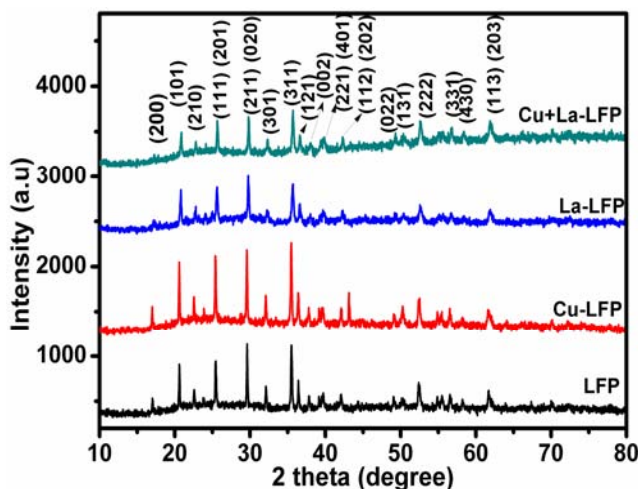

Fig. 1. *XRD pattern of bare and doped LiFePO$_4$ composite materials.*

Table 1. *An estimation of lattice parameter values of prepared materials.*

Sample Name	a (Å)	b (Å)	c (Å)	V (Å³)	Average crystallite size (D) nm
JCPDS 83-2092	10.33	6.010	4.693	291.47	--
LFP	10.3332	6.0064	4.7033	291.91	66
Cu-LFP	10.3324	6.0152	4.7013	292.19	53
La-LFP	10.3283	6.0082	4.6956	291.38	45
Cu+La-LFP	10.3324	6.0222	4.6923	291.97	40

3.2. FT-IR

Fourier transform infrared spectra (FT-IR) is a useful tool to probe the local composition of the surface layer because the vibrations of the molecular units of the $LiFePO_4$ and their composites. Figure 2 illustrate the FT-IR spectra of prepared samples in the range of 4000-400 cm^{-1}. The intramolecular vibrations of the $(PO_4)^{3-}$ appear in the wave number range of 372–1139 cm^{-1} [21]. Symmetric and antisymmetric O–P–O bending modes exist in the range of 372–647 cm^{-1}. Symmetric and antisymmetric P–O stretching modes exist in the range of 945–1140 cm^{-1}. In addition to that, the band at about 685 cm^{-1} is observed in both of the curves, which is assigned to the bending modes of Fe-O-H [21]. The band at 587 cm^{-1} is attributed with the Fe-O stretching mode of the $LiFePO_4$ [22]. The band centered at 1456 cm^{-1} may be described as the vibration of the P–O–Fe and O-H bending vibration tarnished at 1621 cm^{-1}.

3.3. SEM with EDX

The morphological and chemical analyses of the prepared samples were performed using scanning electron microscopic (SEM) with Energy dispersive X-ray spectra (EDX). Figure 3 (a-d) represents the SEM image of bare, copper, lanthanum and copper with lanthanum doped $LiFePO_4$ materials via polyol process. The particle shape and size has been varied with induced the various metal substitution on LFP materials. The plate with rod like particles for bare LFP, rod with spherical particles for copper doped LFP, the spherical particle morphology for Lanthanum doped LFP and irregular inhomogeneous particles for copper with lanthanum co-doped LFP samples has been observed from SEM as shown in Figure 3(a-d). The agglomerated particles form secondary particles, which are independent of substitution level [23].
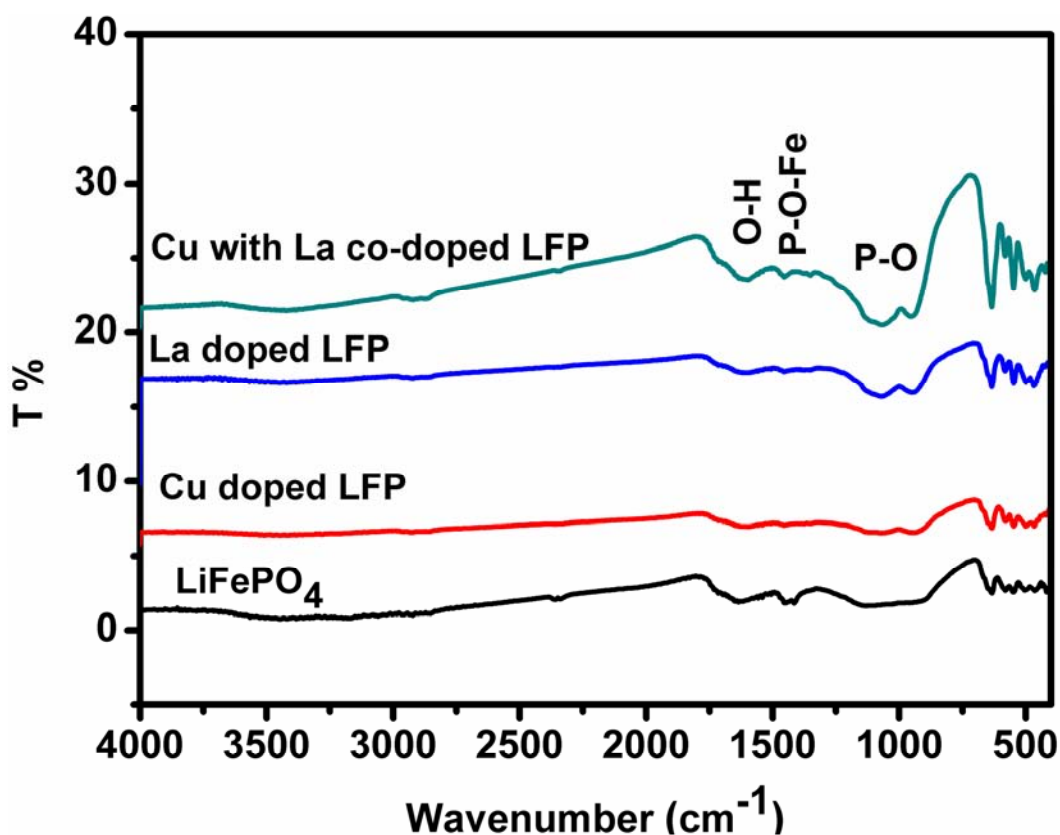

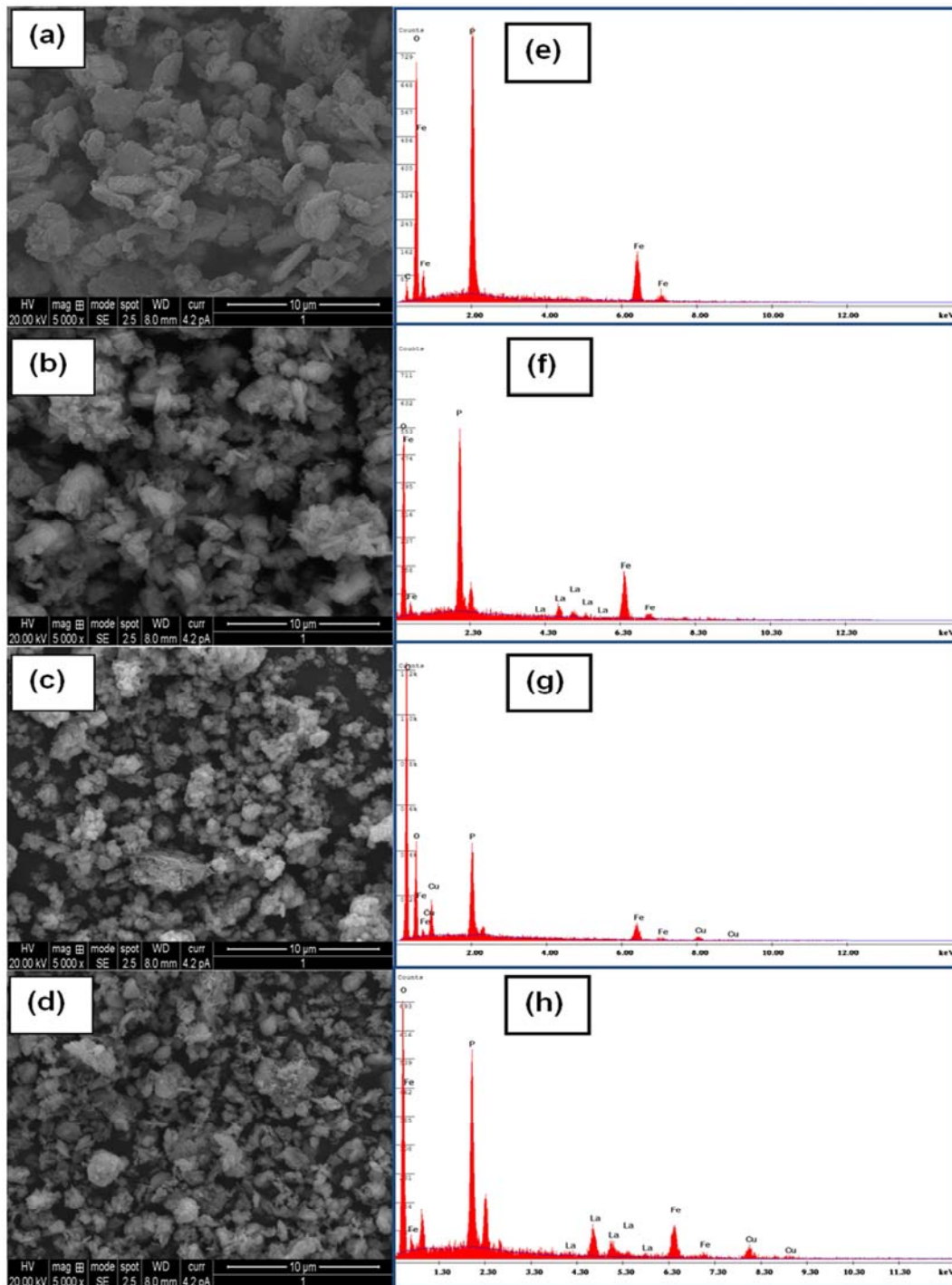***Fig. 2.*** *FT-IR spectra of bare and doped LiFePO₄ composite materials.*

Fig. 3. *(a-d) SEM images and (e-h) EDX spectrum of bare LiFePO₄, Cu-doped LiFePO₄, La-doped LiFePO₄ and Cu with La co-doped LiFePO₄ composite materials, respectively.*

Therefore the different morphological behaviour may be affecting the magnetic properties of the LFP materials. The presence of the all elemental composition has been confirmed by Energy dispersive X-ray spectra as shown in Figure 3(e-h). Hence, the EDX analysis can't detect Li element in the spectrum because it is a light element [24].

3.4. Magnetic Properties-VSM

The magnetic properties were studied to confirm sample purity, transition metal oxidation states and structural ordering. Since magnetic measurements are more sensitive to these issues than X-ray diffraction [25].

The room-temperature specific magnetization (M-H) curves of prepared bare and doped-LiFePO₄ samples are shown in Figure 4. The M-H curve has been analysed by VSM measurement. All the prepared materials are designate that the soft magnetic nature at room temperature. The prepared materials were refluxed at 320°C without annealing process and special environmental.
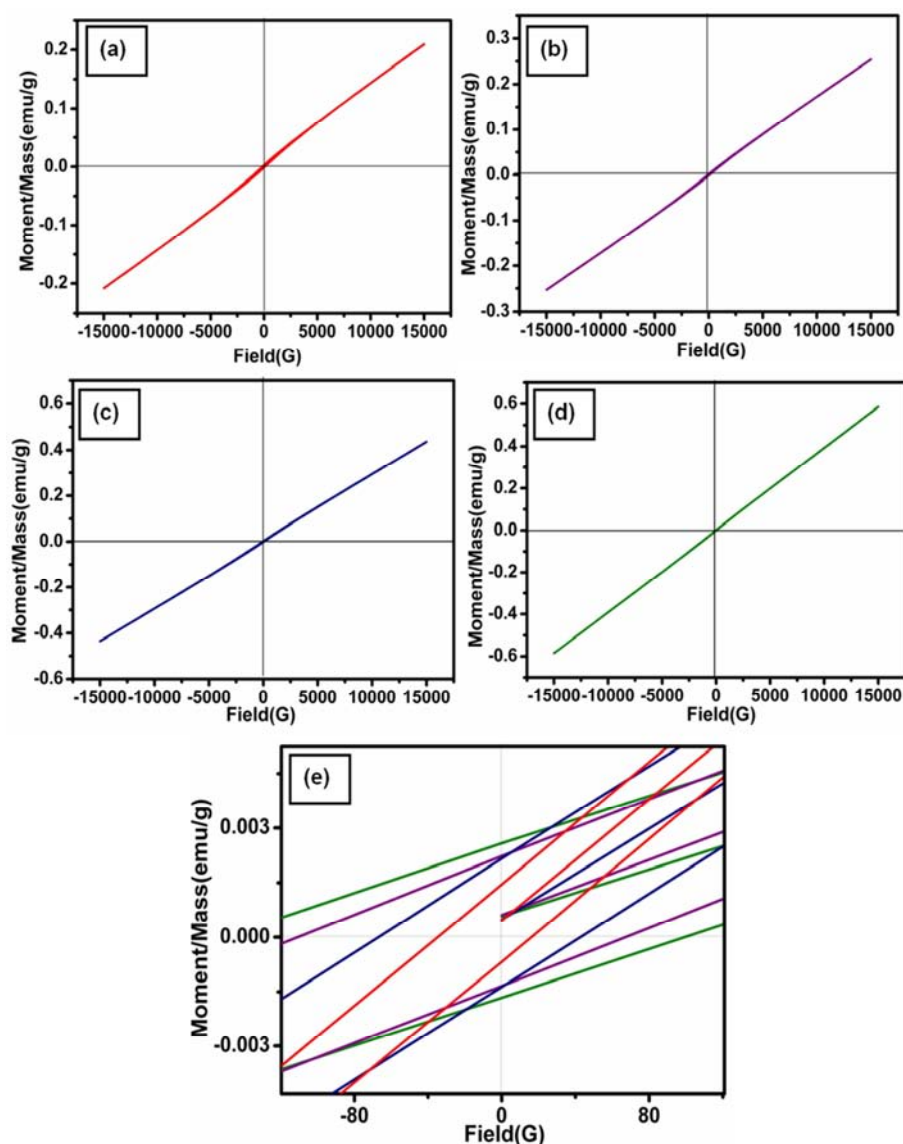
Fig. 4. M-H curve of prepared (a) bare LiFePO$_4$, (b) Cu-doped LiFePO$_4$, (c) La-doped LiFePO$_4$, (d) Cu with La co-doped LiFePO$_4$ composite materials and (e) coercivity enlarged image of all samples, respectively.

It exhibits the spin-glass behaviour with antiferromagnetic nature for all samples [26-28] and the observed values of the Magnetization (M$_s$), coercivity force (Hc$_i$) and retentivity (M$_r$) are shown in Tab. 2. The induced Cu, La and both content on LFP, the coercivity and retentivity values of the prepared samples are slightly decreased, which is consistent with weakening of the antiferromagnetic exchange of metal substitution on LFP.

Table 2. Observed Magnetic Parameters values of prepared materials.

Samples name	Morphological nature SEM image observation	Average crystallite size (D) nm	Coercivity (Hci) (G)	Retentivity (Mr) (×10-3 emu/g)	Magnetization (Ms) (emu/g)
Bare LFP	Plate with rod	66	125.38	2.1227	0.20888
Cu doped LFP	Spherical with rod	53	88.852	1.7854	0.25364
La doped LFP	Spherical	45	54.811	1.7692	0.43589
Cu with La doped LFP	Spherical with rod	40	25.425	1.0670	0.58560

Moreover, the M-H measurements may reveal the presence of magnetic impurity in LFP materials concentration. Also, it can be easily derived the impurity and evaluating the degree of purity of the prepared LiFePO$_4$. The magnetization (M-H) curves of all samples are linear in the magnetic field up to 10 KOe at room temperature. Therefore, the prepared materials

are free from Fe-based magnetic impurities like γ-Fe_2O_3 and Fe_2P phases [29, 30].

4. Conclusion

The phase, local structure of the polyol process prepared LFP and their composites have been explored by XRD and FT-IR analyses. It is an orthorhombic olivine structure and without impurities has been observed. The prepared samples results various shapes of particles with average particle size in the range of 200-100 nm. The magnetic measurements showed that the evidence of spin-glass behaviour with antiferromagnetic nature without magnetic impurities of $LiFePO_4$ at room temperature. However, the dopant Cu, La and both has been reduced the coercivity and retentivity of the LFP materials. This result indicates that the polyol solvent is stabilized the Fe-ion and the magnetizations values changed due to substitution of other metals on LFP without Fe-based magnetic impurities. Moreover, the polyol process is energy-efficient, low cost precursor, significantly less expensive and easier to prepare the nano crystallite-electrode materials.

References

[1] K. T. Lee, J. Cho, Nano Today 6, 28 (2011).

[2] E. Serrano, G. Rus, Javier G –M, Renewable and Sustainable Energy Reviews 13 2373 (2009).

[3] A. K. Padhi, K. S. Nanjundaswamy, and J. B. Goodenough, J. Electrochem. Soc. 144, 1188 (1997).

[4] M. Takahashi, S. Tobishima, K. Takei and Y. Sakurai, J. Power Sources, 97–98, 508 (2001).

[5] S. Liu, H. Yin, H. Wang, J. He, H. Wang, Ceram. Inter. l40, 3325 (2014).

[6] S. Weng, Z. Yang, Q. Wang, J. Zhang, W. Zhang, Ionics, 19, 235 (2013).

[7] S. Yang, P. Y. Zavalij and M. S. Whittingham, Electrochem. Commun. 3, 505 (2001).

[8] K. S. Park, J. T. Son, H. T. Chung, S. J. Kim, C. H. Lee, K. T. Kang and H. G. Kim, Solid State Commun., 129, 311 (2004).

[9] D.-H. Kim, J. K. Kim, Electrochem. Solid State Lett. 9, A439 (2006).

[10] R. Muruganantham, M. Sivakumar, R. Subadevi, Ionics 22, 1557 (2016).

[11] J. Zhang, J. Lu, D. Bian, Z. Yang, Q. Wu, and W. Zhang, Ind. Eng. Chem. Res. 53, 12209 (2014).

[12] C. M. Julien, A. Ait-Salah, A. Mauger, F. Gendron, Ionics 12, 21 (2006).

[13] L. Zhi, D. Nai-Li, K. Zhi-Qi, C. Zhao-Hua, L. Li-Jun, C. Li-Quan, and H. Xue-Jie, Chin. Phys, 13(12), 2158 (2004).

[14] R. P. Santoro, R. E. Newman, Acta Crystallogr. 22, 344 (1967).

[15] F. Croce, A. D. Epifanio, J. Hassoun, A. Deptula, T. Olczac and B. Scrosati, Electrochem. Solid-State Lett., 5, A47 (2002).

[16] N. Jayaprakash, N. Kalaiselvi, P. Periasamy, Int. J. Electrochem. Sci., 3, 476 (2008).

[17] Y-D. Cho, G. T-K. Fey, H-M. Kao, J. Solid State Electrochem 12, 815 (2008).

[18] N. Jayaprakash, N. Kalaiselvi, Electrochem. Commu. 9, 620 (2007).

[19] Y. Xie, H-T. Yu, T-F. Yi, Y-R. Zhu, ACS Appl. Mater. Interfaces 6, 4033 (2014).

[20] M. Yoncheva, V. Koleva, M. Mladenov, M. Sendova-Vassileva, M. Nikolaeva-Dimitrova, R. Stoyanova, E. Zhecheva, J. Mater. Sci, 46, 7082 (2011).

[21] C. M. Burba, R. Frech, Spectrochim Acta A 65, 44 (2006).

[22] S. Zhang, W. Wu, X. Xiao, J. Zhou, F. Ren, C. Jiang, Nanoscale Res. Lett. 6, 89 (2011).

[23] J. Song, L. Wang, G. Shao, M. Shi, Z. Ma, G. Wang, W. Song, S. Liua, C. Wang, Phys. Chem. Chem. Phys., 16, 7728 (2014).

[24] R. Muruganantham, R. Subadevi, M. Sivakumar, Elixir Magnetic Materials 50, 10609 (2012).

[25] F. Omenya, N. A. Chernova, S. Upreti, P. Y. Zavalij, K-W. Nam, X-Q. Yang, and M. S. Whittingham, Chem. Mater., 23, 4733 (2011).

[26] S. Upreti, N. A. Chernova, J. Xiao, J. K. Miller, O. V. Yakubovich, J. Cabana, C. P. Grey, V. L. Chevrier, G. Ceder, J. L. Musfeldt, and M. S. Whittingham, Chem. Mater. 24, 166 (2012).

[27] I. K. Lee, I-B. Shim, and C. S. Kim, J. Appl. Phys. 107, 09A522 (2010).

[28] G. Rousse, J. Rodriguez-Carvajal, S. Patoux and C. Masquelier, Chem. Mater. 15, 4082 (2003).

[29] G. C. Giselle, J. J. Klein, W. H. Schreiner, D. H. Mosca, A. J. A. de Oliveira, A. J. G. Zarbin, J. Colloid and Interface Science 311, 461 (2007).

[30] B. Boonchom, C. Danvirutai, S. Youngme, S. Maensiri, Ind. Eng. Chem. Res. 47, 7642 (2008).